IEEE Photonics Journal
An IEEE Photonics Society Publication

The Polarization Multiplexing Image with a Single Diffractive Optical Element

Volume 9, Number 3, June 2017

Jiazhou Wang
Hui Pang
Axiu Cao
Man Zhang
Ruifeng Kan
Song Hu
Lifang Shi
Qiling Deng

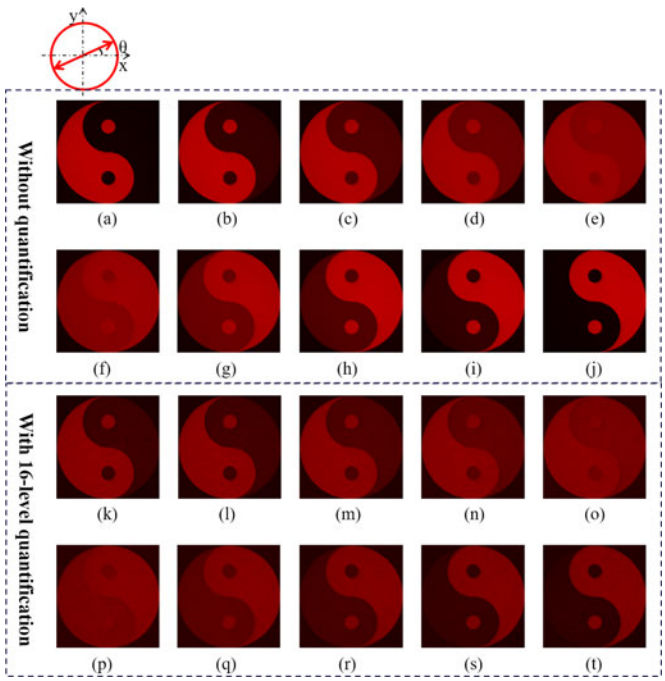

DOI: 10.1109/JPHOT.2017.2703779
1943-0655 © 2016 IEEE

The Polarization Multiplexing Image with a Single Diffractive Optical Element

Jiazhou Wang,[1,2] Hui Pang,[1] Axiu Cao,[1,2] Man Zhang,[1] Ruifeng Kan,[3] Song Hu,[1] Lifang Shi,[1] and Qiling Deng[1]

[1]Institute of Optics and Electronics, Chinese Academy of Sciences, Chengdu 610209, China
[2]University of Chinese Academy of Sciences, Beijing 100049, China
[3]Hefei Institutes of Physical Science, Chinese Academy of Science, Hefei 230031, China

DOI:10.1109/JPHOT.2017.2703779

Manuscript received March 13, 2017; revised April 28, 2017; accepted May 9, 2017. Date of publication May 11, 2017; date of current version May 24, 2017. This work was supported in part by the National Natural Science Foundation of China under Grants 61505214 and 61605211; in part by the Applied Basic Research Programs of Department of Science and Technology of Sichuan Province (Nos. 2016JY0175, 2016RZ0067, 2017JY0058); in part by the Youth Innovation Promotion Association, Chinese Academy of Sciences (CAS); in part by the CAS "Light of West China" Program; and in part by the Key Laboratory of Environmental Optics and Technology, CAS.
Corresponding authors: Lifang Shi and Qiling Deng (e-mail: shilifang@ioe.ac.cn; dengqiling@ioe.ac.cn).

Abstract: The diffractive optical element (DOE) can modulate the light to image in a fixed distance. However, when the wavelength of the light is single and fixed, the imaging is single. In this paper, we proposed a novel architecture to solve this problem. The birefringent material is used as the substrate of the DOE, and the polarization modulation is added in the design of the DOE. The two orthogonally linear polarized lights with the same wavelength modulated by the DOE image differently at the same distance. The imaging of incident light with different polarization is simulated, and the diffraction efficiency and the uniformity are also calculated to demonstrate the validity of this mew method.

Index Terms: Diffractive imaging, holography, theory and design, polarization.

1. Introduction

Diffractive optical elements (DOEs) are key optical components composing of the miniaturized relief structures, enabling the phase modulation of incident lights, which contributes to holographic imaging, focusing and separation of the incident lights. Compared to conventional optical elements, DOE are featured with high miniaturization and integration, yielding high performance in optical systems [1]–[3].

In the traditional design of DOE, the relief structures were designed and fabricated in anisotropic crystal substrate, where different images of the single wavelength at different distances or multiple wavelengths at the same distance were obtained [4]–[7]. However, when the incident light was composed of single and predefined wavelengths, DOE can only produce one phase modulation, which was too simple to meet complex requirements.

To address this issue, the concept of polarization modulation was included in DOE, enabling multiple phase modulations of the incident light at the single wavelength. In 1995, Xu *et al*. proposed a relief structure that was composed of surface-etched birefringent substrates joined face to face where different phase modulations and images of the single wavelength light with two orthogonally linear polarizations were achieved, which, however, suffered from the issue of low diffractive

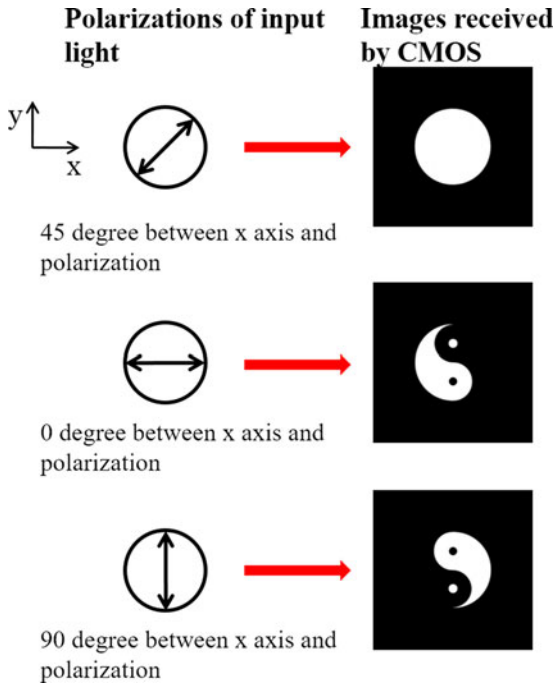

Fig. 1. The ideal output light of PDOE.

efficiency [8]. In 1997, Nieuborg *et al*. proposed a relief structure using gap materials with matching index to increase the diffractive efficiency. However, this structure requested multiple layers, and thus the alignment issue compromised its functionalities [9]. In 2002, Yu *et al*. proposed phase-only polarization multiplexed DOE by including one-dimensional and two-dimensional subwavelength periodic structures, producing limited phase levels [10], [11]. In 2004, Mirotznik *et al*. proposed cell-encoding concepts to fabricate two-dimensional polarization-selective DOE, obtaining nearly an arbitrary number of phase levels, and thus significantly improving diffraction efficiencies [12]. However, because each unit of the structure composed of the periodic striped, it is difficult to ensure the accuracy of etching depth, which limited further improvement in the diffractive efficiency. With the development of the metamaterials, in 2016, Wen *et al*. fabricated meta-surfaces to modulate both left-hand and right-hand circularly polarized lights, obtaining different images in case of single wavelength at the same distance [13]. But the size of the pixel was in the order of one hundred nanometers, and thus electron beam direct writing was requested to fabricate the requested meta-surfaces, leading to high fabrication cost and low production efficiency.

This paper presents a new method using the birefringent material as the substrate to design the polarization DOE (PDOE). In the design process, the structure is designed to realize different phase modulations and different imaging of the incident light with the different polarizations. The two different phase modulations are superposed point by point in design area after calculating. Both of the design method and the parameters selection criterion are given out. On this basis, the structure is designed according to the ideal image of the Taiji diagram. The two orthogonally linear polarized lights modulated by the DOE image differently at the same distance. The polarization modulation of the incident light is achieved. The imaging of the PDOE has high diffraction efficiency and good uniformity, and the fabrication procedure is consistent with the common DOE.

2. Principle

The PDOE can be designed based on the following method. More specifically, ideal images supposed to be generated by the PDOE are shown in Fig. 1, where the fast axis is parallel to the

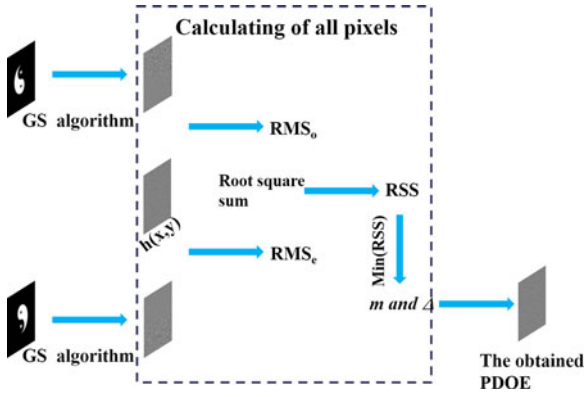

Fig. 2. The flow chart of designed PDOE.

x-axis. If the polarization direction of the incident light to the *x*-axis is 45, the image will be a uniform circular area. If the polarization direction of the incident light to the *x*-axis is 0 (ordinary-polarized) or 90 (extraordinary-polarized), the image will be obtained the left or the right of the Taiji diagram respectively. The different images in the same distance of the lights with the same polarization will be received.

In order to realize different phase modulations of the incident light with different polarizations, the birefringent will be introduced in the design process, and the polarization properties will be considered in the DOE design (see Fig. 2). The left two images represent that the structures have two different phase modulations of the incident light. In order to obtain two different phase modulations, two DOEs will be designed correspondingly to the ordinary- and extraordinary-polarized lights, respectively. In order to superpose two different phase modulations for the ordinary- and extraordinary-polarized lights in a single structure, the design area will be quantified into multiple pixels to enable phase modulations point by point, and the depth of each pixel will be obtained after calculating. The pixel depth of PDOE will be optimized pixel-by-pixel according to the square sum of the phase difference value, and the relief depth distribution of the PDOE will be realized.

In designing diffractive elements, the relationship of the relief distribution h and phase distribution φ was shown as follows,

$$\varphi = 2\pi \frac{h}{\lambda(n-1)} \tag{1}$$

where n is the refractive index of the material for the light with the wavelength of λ. The birefringent material has different refractive index of n_e and n_o for ordinary- and extraordinary-polarized light respectively. The same relief depth of the birefringent phase plate demonstrated different phase modulations for two orthogonally linear polarizations. The distribution of the relief depth of PDOE was h. When the ordinary- and extraordinary-polarized light pass PDOE, two lights had phase distribution ofΦ_o and Φ_e, respectively. When the relief depth of $m\lambda/(n\text{-}1)$ was added to DOE, the phase change of the light with the wavelength of λ was multiplied by 2π, where the imaging was not affected. When the relief depth of $\Delta\lambda/(n\text{-}1)$ was added to DOE, there was a zero-order that was not supposed to. Since Δ within a certain range allowed facial differences, the influence of zero-order can be ignored.

Set the ideal output light field of the ordinary- and extraordinary-polarized light are U_o and U_e respectively. The Gerchberg-Saxton (GS) algorithm was used to design DOE for two polarization states, and the relief depth distributions of the DOE were represented by h_o, and h_e, respectively. Taking h_o as the initial height, the height of each pixel in PDOE was shown in Eq. (2) as follows.

$$h(x, y) = h_o(x, y) + (m + \Delta)\lambda/(n_o - 1) \tag{2}$$

where, m is the integers in the range of [0, M], M is a fixed positive integer, which determines the depth of PDOE. The value of M needs to be determined according to the real quantitative

and processing requirements. Δ is the integer in the range of $[-\delta\%, \delta\%]$ used for regulating facial patterns, h is the relief depth distribution of PDOE, (x, y) is the coordinate of DOE. When the value of δ was properly chosen, the image generated by PDOE of the ordinary-polarization light was almost not affected, and the intensity of zero-order met the imaging needs.

In the design process, according to the required optical results, the proper use of the point-by-point calculations to obtain the right depth value for each pixel was a key problem. Since the values of m and Δ were not determined for each pixel in the Eq. (2), they need to be quantified using the h_e, as shown in Eq. (3),

$$\begin{aligned} RMS_o &= \mathrm{mod}_\lambda\left[h(x, y) \times (n_o - 1)\right] - h_o(x, y) \times (n_o - 1); \\ RMS_e &= \mathrm{mod}_\lambda\left[h(x, y) \times (n_o - 1)\right] - h_e(x, y) \times (n_e - 1); \end{aligned} \tag{3}$$

where the RMS_o and RMS_e represent equivalent phase differences between PDOE and the single DOE for the ordinary- and extraordinary-polarized light, respectively. Mod_a (b) represents a seeking complementary function of a for b. When the root square sums (RSS) of the RMS_o and RMS_e were minimized, the values of m and Δ were obtained. RSS was calculated by Eq. (4).

$$RSS = \sqrt{RMS_o^2 + RMS_e^2} \tag{4}$$

m and Δ were then substituted into Eq. (2), leading to the quantification of each pixel height of PDOE. In order to evaluate the results more accurately, two evaluation functions were introduced, which were diffraction efficiency of Eff and root mean square error of MSE as follows:

$$\begin{aligned} Eff &= \frac{\sum I_t}{\sum I_{all}}; \\ MSE &= \sqrt[2]{\frac{\sum\sum\left(\left|E_t(x, y)\right| - \left|E_m(x, y)\right|\right)^2}{n}}; \end{aligned} \tag{5}$$

where I_t is the intensity of the signal area imaged by the incident light passing through PDOE, I_{all} is the total intensity of incident light from the PDOE, E_t is the light distribution generated by PDOE, E_m is the target light distribution, and n is the number of the pixels. The simulation results were analyzed quantitatively by using these two evaluation functions.

3. Parameters Determination

There were two uncertain parameters (M and δ) in the PDOE design process, which determined the image qualities directly and were quantified by the evaluation functions.

Firstly, the value of M was quantified. In the simulation, the range of Δ was within $[-20\%, 20\%]$, and the range of m was within $[0, M]$. In the simulation of ten times, the values of the M were 1, 2, 3, . . . , 10, respectively. The diffraction efficiency Eff and root mean square error MSE were used to evaluate the image quality of the PDOE which are unquantized and quantized. The simulated results are shown in Fig. 3.

Fig. 3(a) shows the relationship between the diffraction efficiency of the ordinary- and extraordinary-polarized lights and M. The yellow line shows the result of the incident light with ordinary-polarization and PDOE without quantification. The blue line shows the result of the incident light with extraordinary-polarization and PDOE without quantification. The red line shows the result of the incident light with ordinary-polarization and PDOE with 16-level quantification. The green line shows the result of the incident light with extraordinary-polarization and PDOE with 16-level quantification. Fig. 3(b) shows that the relationship between the root mean square error of the ordinary- and extraordinary-polarized light and M. The yellow line shows the result of the incident light with ordinary-polarization and PDOE without quantification. The blue line shows the result of the incident light with extraordinary-polarization and PDOE without quantification. The red line shows the result of the incident light with ordinary-polarization and PDOE with 16-level quantification. The green line shows the result of the incident light with

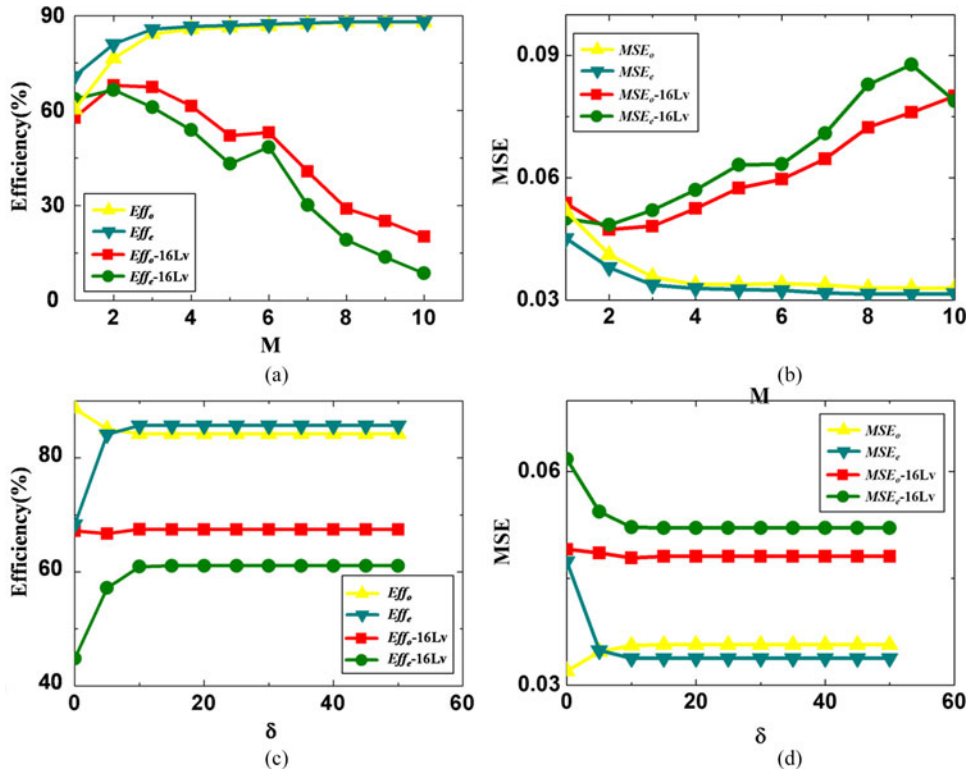

Fig. 3. Relationships between diffraction efficiency and M (a) and the root mean square error and M (b); Relationships between diffraction efficiency and δ (a) and the root mean square error and δ (b).

extraordinary-polarization and PDOE with 16-level quantification. It was observed that when PDOE was not quantified, the increase of *m* lead to 1) an increase in the range of *M*, an increase in the diffraction efficiency, a decrease in the root mean square error, and an increase in the image quality. When PDOE was quantified to be 16 levels, in case of $M = 2$, the average value of the diffraction efficiency was maximized and the root mean square error was minimized. When *M* was not high enough, the degree of iteration freedom was limited, leading to the compromise of the image qualities. With the increase of *M*, the maximum height of PDOE was increased, making the structure of the quantized PDOE more different. In the aforementioned two cases, in case of $M = 2$, the image quality was the best.

Aforementioned analysis indicated that the image quality was the best in case of $M = 2$. Under the same simulation conditions, the value of *M* is 2, and the range $[-\delta\%, \delta\%]$ of Δ is different. The value of δ were 0, 5, 10, . . . , 50 respectively to find out the relationship between the image quality and the value of δ. The simulation results are shown in Fig. 3

Fig. 3(c) shows that the relationship between the diffraction efficiency of the ordinary- and extraordinary-polarized lights and δ. The yellow line shows the result of the incident light with ordinary-polarization and PDOE without quantification. The blue line shows the result of the incident light with extraordinary-polarization and PDOE without quantification. The red line shows the result of the incident light with ordinary-polarization and PDOE with 16-level quantification. The green line shows the result of the incident light with extraordinary-polarization and PDOE with 16-level quantification. Fig. 3(d) shows that relationship between the root mean square error of the ordinary- and extraordinary-polarized light and δ. The yellow line shows the result of the incident light with ordinary-polarization and PDOE without quantification. The blue line shows the result of the incident light with extraordinary-polarization and PDOE without quantification. The red line shows the result of the incident light with ordinary-polarization and PDOE with 16-level quantification. The green line shows the result of the incident light with extraordinary-polarization and PDOE

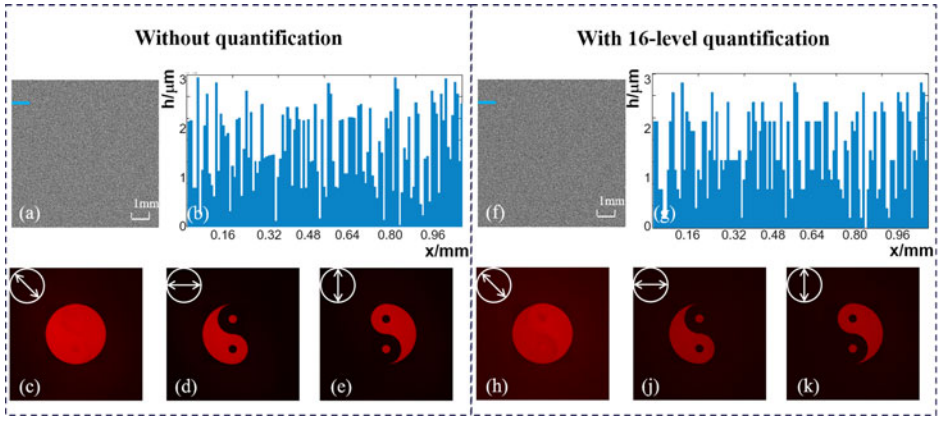

Fig. 4. (a) and (b) Obtained relief depth distributions of PDOE without quantification and the simulated output light with the polarization angle θ to the fast axis, (c) $\theta = 45$, (d) $\theta = 0$, ordinary polarized light, (e) $\theta = 90$, extraordinary polarized light. (f) and (g) Obtained relief depth distributions of PDOE without quantification and the simulated output light with the polarization angle θ to the fast axis, (h) $\theta = 45$, (i) $\theta = 0$, ordinary polarized light, (j) $\theta = 90$, extraordinary polarized light.

with 16-level quantification. In case of δ<10, the image quality of the ordinary-polarized light was significantly better than extraordinary-polarized light, indicating that the optimization of the freedom degree was not high and the structure did not function in the optimized case. In case of $\delta \geq 10$, the degree of iteration freedom increased with the increase of δ. When δ was increased to a certain degree, the degree of iteration freedom demonstrated saturation. The image quality of the ordinary- and extraordinary-polarized light was stable and comparable. These results indicate that under the premise of ensuring image qualities, the height of PDOE should be as low as possible, and thus the value of δ was optimized as 10.

4. Simulation

After parameter determination, the algorithm was realized using MATLAB to conduct simulations. The substrate material was chosen as YVO4, and its birefringence of n_o and n_e were 1.9929 and 2.2154, respectively, with the wavelength of the incident light chosen 632nm.The distance between PDOE and the imaging surface was 0.7 m. The number of sampling pixels in PDOE was 1024 $\times$ 1024, and size of each pixel was 8 μm $\times$ 8 μm. According to the design flow process, the simulation was conducted and the results were shown in Fig. 4.

It was observed that the highest relief depth of PDOE was 2.657 μm (see Fig. 4(a), (b), (f) and (g)). The output of the linear polarized light from PDOE was shown with three polarization directions of $\theta = 45$ to the fast axis in Fig. 4(c) and (h), ordinary polarized light in (d) and (i), and extraordinary polarized light in (e) and (j), respectively. From the simulation results, orthogonally linear polarized lights passed through the phase plate producing different images, and the intensity distribution of each image was featured with high uniformity. In the event that the structure of PDOE wasn't quantified, when incident light was the ordinary polarized light, the diffraction efficiency was quantified as 84.21%, and the root mean square error was quantified as 0.0357. when incident light was the extraordinary polarized light, the calculated diffraction efficiency was quantified as 85.69%, and the root mean square error was quantified as 0.0338. In the event that the structure of PDOE was quantified, when incident light was the ordinary polarized light, the diffraction efficiency was quantified as 67.44%, and the root mean square error was quantified as 0.0481. when incident light was the extraordinary polarized light, the calculated diffraction efficiency was quantified as 61.05%, and the root mean square error was quantified as 0.0521. Even the result of simulation imaging or evaluation functions could be recognized that the two orthogonally linear imaging has ideal diffraction efficiency and low uniformity error. These results also suggested that the polarization of the imaging area has negligible interactions (see Fig. 5).

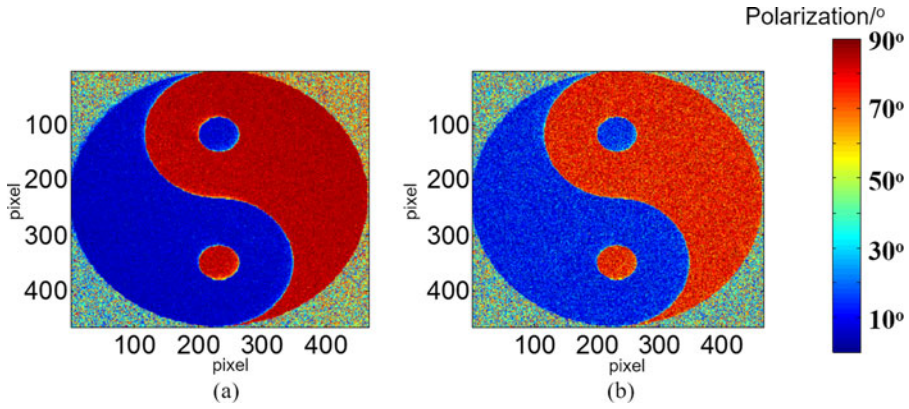

Fig. 5. The polarization distribution of the imaging area from PDOE without quantification (a) and with quantification (b).

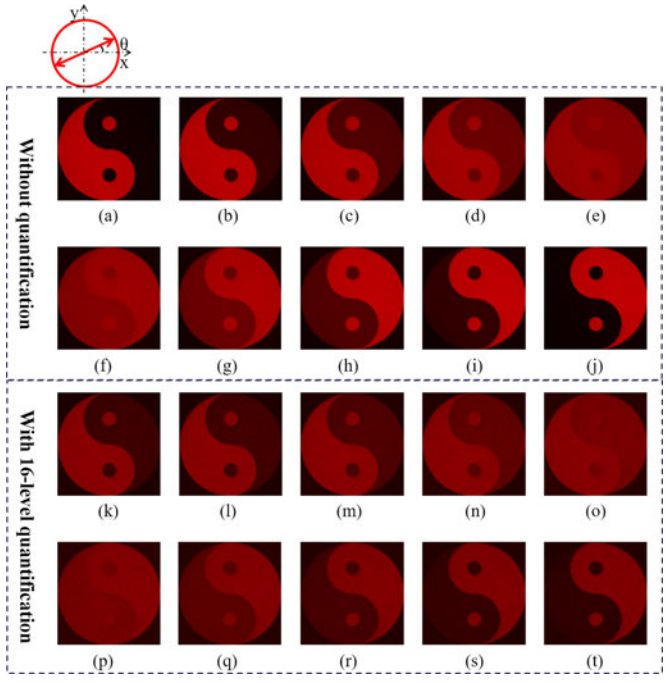

Fig. 6. Light field distributions of the incident lights with different polarization directions (θ) through the phase plate. The phase plate without quantification: (a) $\theta = 0$, (b) $\theta = 10$, (c) $\theta = 20$, (d) $\theta = 30$, (e) $\theta = 40$, (f) $\theta = 50$, (g) $\theta = 60$, (h) $\theta = 70$, (i) $\theta = 80$, (j) $\theta = 90$. The phase plate with 16-level quantification: (k) $\theta = 0$, (l) $\theta = 10$, (m) $\theta = 20$, (n) $\theta = 30$, (o) $\theta = 40$, (p) $\theta = 50$, (q) $\theta = 60$, (r) $\theta = 70$, (s) $\theta = 80$, (t) $\theta = 90$.

As shown in Fig. 5, the images produced by PDOE had high diffraction efficiency and uniformity. When there was no overlap in the target field, the impact of the vector superposition was negligible, and the polarization distribution of images was consistent with the polarization of the incident light. When there was overlap of target fields, the vectors of the light fields were added together according to the amplitude ratio, and the optional polarization distribution was realized. However, since the phase was not modulated, the polarization of the light field was an elliptical polarization with random phases. The light field distributions of the incident light with different polarization directions through the phase plate were shown in the Fig. 6.

It was observed that the change of the incident light's polarization angles lead to the light field gradients. According to the Jones matrix, the linear polarized light can be decomposed into two

polarized lights with the parallel and the perpendicular polarization to the fast axis respectively, and the two lights were combined by applying the principle of vectorial resultant. The angle of the incident light determined the intensity ratio of the two decomposed polarized lights directly. With the different angles of the incident lights, the intensity distributions of images changed gradually. The different images at the fixed distance for the lights with single and fixed wavelengths were obtained by modulating the polarization of the incident lights, validating the feasibility of this method.

5. Conclusion

In this paper, a method was proposed to design polarization DOE where the image from the PDOE was not single at the fixed distance for the light with the same wavelength. Two orthogonally linear polarized lights with the same wavelength modulated by DOE formed images differently at the same distance. The images demonstrated high diffractive efficiencies and low uniformity errors. The validity of the PDOE was demonstrated and the range of DOE applications was expanded, which may include security and encryption.

Acknowledgment

The authors would like to thank the anonymous reviewers for their valuable suggestions. They would also like to thank their colleagues for their discussions and suggestions to this paper.

References

[1] J. Amako, K. Nagasaka, and E. Fujii, "Direct laser writing of diffractive array illuminators operable at two wavelengths," *Proc. SPIE*, vol. 4416, pp. 360–363, 2001.
[2] F. Yaras, H. Kang, and L. Onural, "State of the art in holographic displays: A survey," *J. Display Technol.*, vol. 6, no. 10, pp. 443–454, 2010.
[3] H. Pang, S. Y. Yin, Q. L. Deng, Q. Qiu, and C. L. Du, "A novel method for the design of diffractive optical elements based on the rayleigh-sommerfeld integral," *Opt. Lasers Eng.*, vol. 70, pp. 38–44, 2015.
[4] M. Makowski, M. Sypek, and A. Kolodziejczyk, "Colorful reconstructions from a thin multi-plane phase hologram," *Opt. Exp.*, vol. 16, no. 15, pp. 11618–11623, 2008.
[5] C. F. Ying, H. Pang, C. J. Fan, and W. D. Zhou, "New method for the design of a phase-only computer hologram for multiplane reconstruction," *Opt. Eng.*, vol. 50, no. 50, pp. 301–301, 2011.
[6] A. Jesacher, S. Bernet, and M. Ritschmarte, "Colour hologram projection with an SLM by exploiting its full phase modulation range," *Opt. Exp.*, vol. 22, no. 17, pp. 20530–20541, 2014.
[7] J. Z. Wang, H. Pang, M. Zhang, L. F. Shi, A. X. Cao, and Q. L. Deng, "Design method of multi-wavelength diffractive optical element," *Acta Optica Sinica*, vol. 35, no. 10, 2015, Art. no. 1005002.
[8] F. Xu, J. E. Ford, and Y. Fainman, "Polarization-selective computer-generated hologram: Design, fabrication, and application," *Appl. Opt.*, vol. 34, no. 2, pp. 256–265, 1995.
[9] N. Nieuborg, A. Kirk, B. Morlion, H. Thienpont, and I. Veretennicoff, "Polarization-selective diffractive optical elements with an index-matching gap material," *Appl. Opt.*, vol. 36, pp. 4681–4685, 1997.
[10] W. J. Yu, T. Konishi, T. Hamamoto, H. Toyota, T. Yotsuya, and Y. Ichioka, "Polarization-mltiplexed diffractive optical elements fabricated by subwavelength structures," *Appl. Opt.*, vol. 41, no. 1, pp. 96–100, 2002.
[11] F. Xu, R. Tyan, P. Sun, Y. Fainman, C. Cheng, and A. Scherer, "Form-birefringent computer-generated holograms," *Opt. Lett.*, vol. 21, pp. 1513–1515, 1996.
[12] M. S. Mirotznik, D. M. Pustai, D. W. Prather, and J. N. Mait, "Design of two-dimensional polarization-selective diffractive optical elements with form birefringent microstructures," *Appl. Opt.*, vol. 43, no. 32, pp. 5947–5954, 2007.
[13] D. D. Wen *et al.*, "Helicity multiplexed broadband metasurface holograms," *Nature Commun.*, vol. 6, 2015, Art. no. 8241.